Check for updates

Received: 30 December 2020 | Revised: 9 February 2022 | Accepted: 10 February 2022

DOI: 10.1002/eqe.3625

RESEARCH ARTICLE

WILEY

Impact of soil-structure interaction on the effectiveness of Tuned Mass Dampers

Davide Noè Gorini[1] | **Corrado Chisari**[2]

[1]Department of Structural and Geotechnical Engineering, Sapienza University of Rome, Rome, Italy

[2]Department of Architecture and Industrial Design, University of Campania "Luigi Vanvitelli", Italy

Correspondence
Davide Noè Gorini, Department of Structural and Geotechnical Engineering, Sapienza University of Rome, Rome, Italy.
Email: davideno.gorini@uniroma1.it

Abstract

Tuned Mass Dampers (TMDs) can represent an attracting solution to mitigate vibrations of a structure under seismic excitation, but their effectiveness can be considerably altered by the dynamic interaction with the foundation soil. The available design criteria for TMDs do not account for these effects and can therefore lead to a non-optimised structural performance. In this paper an investigation on the dynamic interaction of the TMD with the whole soil-structure system is presented, with the objective of highlighting the system parameters governing the response and the effectiveness of the device as seismic protection. An interpretative model of the soil-structure-TMD system expressed in a rigorous non-dimensional form is proposed, and an extensive global sensitivity analysis on its performance under harmonic loading is carried out. The identification of the typical performance regions shows that the seismic effectiveness of a TMD is mainly controlled by a limited number of parameters describing the structural behaviour and the soil-structure interaction, such as the structure-to-soil relative stiffness and those governing foundation rocking. The non-dimensional system parameters leading to either a favourable or detrimental effect on the TMD performance due to soil-structure interaction are also identified, and two design methodologies proposed in the literature are critically assessed in light of the framework proposed.

KEYWORDS

foundation rocking, global sensitivity analysis, governing parameters, non-dimensional formulation, soil-structure-TMD interaction

1 | INTRODUCTION

Tuned Mass Dampers (TMDs) are passive devices able to control vibrations in structures. In their most basic configuration, a TMD is constituted of a mass connected to the main structure by means of translational linear springs and dampers. By correctly designing the number of the devices and their position within the structure and tuning the characteristics of the mass and the connecting elements, that is, their stiffness and damping coefficients, it is possible to significantly decrease the accelerations and deformations of the structure, either in case of harmonic loading due to machinery or random vibrations induced by wind or ground motion.[1] In particular, this allows for an effective seismic enhancement

This is an open access article under the terms of the Creative Commons Attribution License, which permits use, distribution and reproduction in any medium, provided the original work is properly cited.

© 2022 The Authors. *Earthquake Engineering & Structural Dynamics* published by John Wiley & Sons Ltd.

of existing structures and design of new ones without resorting to more expensive base isolation or visually impacting viscous or hysteretic damping systems.

Optimal tuning of a TMD is generally related to the significant natural frequencies of the structure. A widely used criterion was proposed by Den Hartog,[2] which provides the optimal analytical solutions for the mass, stiffness and damping of a TMD used in a single-degree-of-freedom (SDOF) system, having fixed base and subjected to harmonic excitation. In Den Hartog's criterion, the optimal performance of the device is controlled by three non-dimensional parameters: the damping ratio $\xi_{TMD} = c_{TMD}/(2 \times m_{TMD} \times \omega_{TMD}) = \{6 \times \mu/[8 \times (1+\mu) \times (2-\mu)]\}^{0.5}$, the frequency ratio $\alpha = \omega_{TMD}/\omega_s = 1/(1+\mu) \times [(2-\mu)/2]^{0.5}$, and the mass ratio $\mu = m_{TMD}/m_s$, where m_{TMD}, ω_{TMD}, c_{TMD} are the TMD mass, circular frequency and damping coefficient, respectively, and ω_s is the fundamental circular frequency of the structure. The mass ratio is usually assumed as an input in the design as is mainly dictated by practical needs, whereas the other two parameters are obtained accordingly. While this criterion ensures the minimisation of deformation in the SDOF under harmonic loading, several studies have shown that its effectiveness may no more be optimal in case of seismic loading[3] or when the linear SDOF approximation is not acceptable.[4] Afterwards, several other studies were proposed for optimal tuning and location of single or multiple TMDs, mainly based on numerical approaches.[3,5–8] Notwithstanding, because of its simplicity and theoretically founded assumptions, Den Hartog's formulation is still the reference in the design of TMDs. Moreover, although strictly speaking the TMD design should depend on the variable frequency content of a natural earthquake, Den Hartog's criterion has proved a near-optimal solution even in the case of pulse-like input.[9]

One of the cases where the SDOF approximation is not acceptable is when soil-structure interaction cannot be neglected, for which the available solutions may lead to detuning of the TMD from the dynamic response of the coupled soil-structure system. This effect was recognised in some analytical studies and verified through experimental evidence. In Wu et al.[10], a frequency-independent numerical structural model was used to analyse the influence of soil-structure interaction on the TMD effectiveness. It was highlighted that a coupled dynamic response between the soil and the structure can jeopardise the effectiveness of a damper system mounted on the top of the structure. Similar conclusions were drawn by Takewaki[11], who proposed an analytical method for optimal placement of viscous dampers in linear-elastic building structures equipped with a TMD and resting on a frequency-independent, horizontal spring-dashpot element simulating soil-structure interaction. A numerical structural model with frequency-dependent soil-structure effects was then proposed by Ghosh and Basu[12], using the tabular solutions provided by Wong and Luco[13] for the horizontal and rotational impedance functions, which were calibrated considering three values of the soil stiffness. Using the analytical solutions provided by Den Hartog[2], it was therein proposed to tune the device to the fundamental frequency of the soil-structure system. Liu et al.[14] developed a mathematical model to predict wind-induced oscillations of a high-rise building with a TMD installed on top and accounting for the soil compliance. The frequency-independent expressions proposed by Wolf[15] were used to determine the swaying and rocking springs and dashpots for three soil cases. Some optimisation methods were also developed by Farshidianfar and Soheili[16–18], Bekdas and Nigdeli[19] and Salvi et al.[20] for the design of TMDs accounting for soil-structure interaction, referring to specific soil-structure layouts.

A means for limiting TMD detuning due to soil-structure interaction is represented by the introduction of a multiple TMD (MTMD) in the structural layout. In this regard, the numerical studies performed by Wang and Lin[21], Li et al.[22], and Li[23] showed that a proper frequency-spacing of the MTMD can control the multi-resonance features of a soil-structure system and the effect of torsional deformation modes. In this regard, a first experimental study was carried out by Jabary and Madabhushi[24] using the geotechnical centrifuge,[25] considering a two-degrees-of-freedom system equipped with a single or double TMD and resting on a sandy soil. In the mentioned paper, the greater efficiency of a double TMD to avoid detuning due to soil-structure interaction and the relevance of foundation rocking was demonstrated. In recent years, several variations of the original idea have been proposed to increase the effectiveness and robustness of TMDs: large mass ratio TMDs,[26] pendulum TMDs with friction,[27] tuned inerter dampers,[28–29] steel frames with aseismic floors.[30] Also in these studies, interaction with soil is generally ignored.

With the aim of defining a more general framework for the study of the effects induced by soil-structure interaction on the seismic performance of TMDs, Gorini and Chisari[31] proposed non-dimensional performance curves relating the effectiveness of the device to the structure-to-soil relative stiffness, as a central factor influencing the TMD performance. A large variability of the relative stiffness was therein taken into account, considering a TMD designed according to the solutions proposed by Den Hartog[2] and by Ghosh and Basu.[12] In this paper a comprehensive study on the effect of the soil-structure interaction in the performance of TMDs is carried out. A general non-dimensional framework is proposed and validated referring to a real case study. The governing, non-dimensional parameters controlling the TMD performance in a generic, linear soil-structure system are identified and their effect assessed through the use of global sensitivity analysis methodologies. The performance of the design methods proposed by Den Hartog,[2] for fixed-base structures, and Ghosh

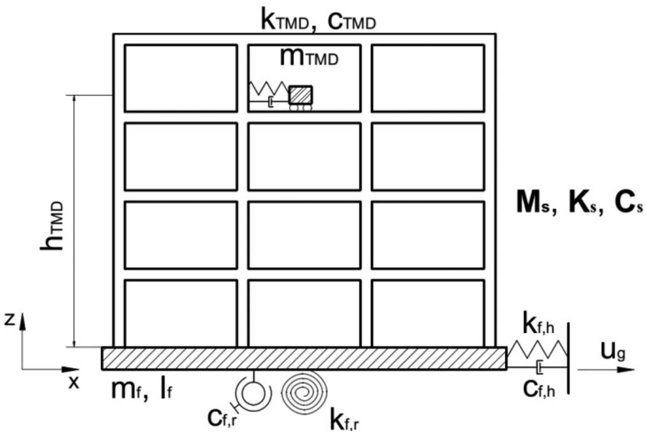

FIGURE 1 Schematic layout of a planar structure equipped with a Tuned Mass Damper and resting on horizontal and rotational dynamic impedance functions

and Basu,[12] for coupled soil-structure systems, are investigated. The regions of the parameter space where the methods provide conservative and un-conservative results are identified and relevant features of the response are highlighted.

2 | EQUATIONS OF MOTION FOR A LINEAR SOIL-STRUCTURE-TMD SYSTEM

Figure 1 depicts a linear soil-structure-TMD system, composed of a planar structure equipped with a TMD and resting on a rigid shallow foundation subjected to horizontal ground motion $u_g(t)$ along X. The structure is characterised by its mass, stiffness and damping matrices, M_s, K_s and C_s, respectively. The soil-structure interaction effects are reproduced by a diagonal dynamic impedance matrix,[32] that can be modelled as two sets of translational and rotational spring-dashpot elements connected to the foundation of mass m_f and moment of inertia I_f, the latter considered around an axis parallel to the global direction Y and passing by its centroid projection on the base. The spring-dashpot elements are characterised by frequency-dependent elastic stiffnesses $k_{f,h}$ and $k_{f,r}$ in the translational and rotational directions, respectively, and damping coefficients $c_{f,h}$ and $c_{f,r}$. These properties are a function of the soil mass density ρ_s, the shear wave velocity V_s of soil and the semi-length of the foundation in the X and Y directions, $L_{f,x}$ and $L_{f,y}$ (Y-axis indicates the out of plane direction).

The structure is equipped with a TMD of mass m_{TMD} placed at an elevation h_{TMD} with respect to the foundation level and connected to the structure by a spring with stiffness k_{TMD}, placed in parallel with a dashpot of coefficient c_{TMD}. The TMD is constrained to move in the horizontal, X direction only. As a simplifying hypothesis, it is assumed that the structure deforms proportionally to its first mode of vibration, Φ_1, normalised with respect to the structural mass. Under this assumption the structure can be reduced to a SDOF system. The motion of this system induced by a horizontal acceleration $\ddot{u}_g$ applied to the base is described by the following system of equations (with dots indicating derivatives with respect to time):

$$M\ddot{u} + C\dot{u} + Ku = -Mi\ddot{u}_g \tag{1}$$

in which the displacement vector $u = [u_0(t)\ \varphi_0(t)\ v(t)\ \Delta u_{TMD}(t)\,]^T$ collects the degrees of freedom of the system, that is, the horizontal displacement and rotation of the foundation, $u_0(t)$ and $\varphi_0(t)$ respectively, the amplitude of the modal shape $v(t)$ and the relative displacement $\Delta u_{TMD}(t)$ of the TMD with respect to the structure at the same elevation. The mass matrix of the soil-structure-TMD system is symmetric, positive definite and reads:

$$M = \begin{pmatrix} m_s + m_f + m_{TMD} & m_s h_{G,s} + m_{TMD} h_{TMD} & \sqrt{m_m} + m_{TMD}\phi_1(h_{TMD}) & m_{TMD} \\ Sym & r_g^2 m_s + I_f + m_{TMD} h_{TMD}^2 & h_m\sqrt{m_m} + m_{TMD} h_{TMD}\,\phi_1(h_{TMD}) & m_{TMD} h_{TMD} \\ Sym & Sym & 1 + m_{TMD}\,[\phi_1(h_{TMD})]^2 & m_{TMD}\phi_1(h_{TMD}) \\ Sym & Sym & Sym & m_{TMD} \end{pmatrix} \tag{2}$$

in which m_s is the total mass of the structure and m_m its effective modal mass: using mass-normalisation, the participation factor of the first mode is $M_{\phi s} = \sqrt{m_m}$; $h_{G,s} = S_s/m_s$ and S_s represent respectively the elevation of the centre of mass and the first moment of mass of the structure, the latter referred to the foundation base; $r_g = \sqrt{I_s/m_s}$, where I_s is the moment of inertia of the structure with respect to an axis parallel to Y and passing by the base; $h_m = z^T M\phi_1/1^T M\phi_1$ defines the effective modal height of the structure; the term $\phi_1(h_{TMD})$ is the modal displacement in correspondence of the TMD.

The damping and stiffness matrices are given below:

$$C = \text{diag}\left(c_{f,s} \quad c_{f,r} \quad c_{\phi s} \quad c_{TMD}\right) \tag{3}$$

$$K = \text{diag}\left(k_{f,s} \quad k_{f,r} \quad k_{\phi s} \quad k_{TMD}\right) \tag{4}$$

in which $k_{\phi s} = {\phi_1}^T K_s\ \phi_1 = \omega_s^2$ is the modal stiffness of the structure, equal to the square of its fundamental circular frequency, ω_s, and $c_{\phi s} = {\phi_1}^T C_s\ \phi_1$ is the damping coefficient of the structure associated with the first modal shape; finally, $i = [1\ 0\ 0\ 0]^T$. In this paper, the case of harmonic time history applied to the base is considered, expressed in the form $u_g = A_0 \sin(\omega_i t)$, where u_g is the input displacement at the base, A_0 and ω_i are the relative amplitude and circular frequency, respectively.

Because the assumption of linear behaviour, it is convenient to divide both members of the equation of motion, Equation 1, by the amplitude of the input, A_0. In this manner, the vector of the output quantities reads:

$$U = u/A_0 = \left[u_0(t) \quad \varphi_0(t) \quad v(t) \quad \Delta u_{TMD}(t)\right]^T/A_0 = \left[U_0(t) \quad \Phi_0(t) \quad \bar{U}(t) \quad \Delta U_{TMD}(t)\right]^T \tag{5}$$

in which $U_0(t)$ and $\Delta U_{TMD}(t)$ are non-dimensional, while the dimensions of $\bar{U}(t)$ and $\Phi_0(t)$ are $M^{0.5}$ and L^{-1} (M = mass; L = length), respectively, as a consequence of the mass normalisation of the modal shape used in this study.

3 | NON-DIMENSIONAL FORMULATION

3.1 | Physical quantities and non-dimensional groups

The physical quantities having a role in the equations of motion are listed in Table 1. By considering the foundation as a continuous slab, m_f and I_f can be easily derived knowing its mass density, ρ_c, plan dimensions, $L_{f,x}$ and $L_{f,y}$, and depth d_w.

With the aim of developing a general formulation highlighting the relevant parameters governing linear, dynamic soil-structure-TMD interaction, a non-dimensional formulation was developed. Following Buckingham pi-theorem, the dynamic response of the system can be completely described by the 19 non-dimensional groups reported in Table 2. The groups have a clear physical meaning and most of them are used in the literature to characterise the soil-structure interaction effects and the seismic performance of structures equipped with a TMD. In detail, groups G_1-G_3 are the basic parameters for the design of TMDs,[2] commonly referred to as mass, frequency and damping ratio. Group G_4 represents the elevation of the TMD normalised with respect to the fundamental modal height of the structure. Group G_5 controls the geometry of the foundation, while an indicator of the relative stiffness between the structure and the soil is given by G_6.[33] Group G_7 represents the slenderness of the system,[33] while G_8 represents the ratio between the total structural mass and the mass of the idealised volume of soil interacting with it. Groups G_{10}-G_{13} characterise the equivalent SDOF system representing a generic structural layout in terms of damping ratio, participating mass and geometrical features. In G_{14} the foundation mass density is normalised with respect to the modal characteristics of the structure. Group G_{15} represents the dynamic interaction between the input motion and the response of the structure. Lastly, the non-dimensional response quantities, R_1-R_4, represent the dynamic amplification of the horizontal displacements of the structure (R_1), of the TMD (R_2), of the foundation (R_3) and the amplification of the foundation rotation (R_4).

TABLE 1 Physical quantities of a linear soil-structure-TMD system

	Number	Symbol	Dimension	Description
Structure	1	$\boldsymbol{m}_{\mathrm{s}}$	M	*Mass of the structure*
	2	$\boldsymbol{m}_{\mathrm{m}}$	M	*Modal mass of the structure*
	3	ω_{s}	1/T	*Fundamental circular frequency of the structure*
	4	$\boldsymbol{c}_{\phi\mathrm{s}}$	M/T	*Damping coefficient of the structure*
	5	$\boldsymbol{h}_{\mathrm{m}}$	L	*Modal height of the structure*
	6	$\boldsymbol{h}_{\mathrm{G,s}}$	L	*Barycentre height of the structure*
	7	$\boldsymbol{r}_{\mathrm{g}}$	L	*Radius of gyration of the structure*
TMD	8	$\boldsymbol{m}_{\mathrm{TMD}}$	M	*Mass of the TMD*
	9	$\boldsymbol{h}_{\mathrm{TMD}}$	L	*Height of the TMD*
	10	$\boldsymbol{k}_{\mathrm{TMD}}$	M/T^2	*Stiffness of the TMD*
	11	$\boldsymbol{c}_{\mathrm{TMD}}$	M/T	*Damping coefficient of the TMD*
Soil-foundation	12	ρ_{s}	M/L^3	*Mass density of soil*
	13	$\boldsymbol{V}_{\mathrm{s}}$	L/T	*Shear wave velocity of soil*
	14	ρ_{c}	M/L^3	*Mass density of the foundation*
	15	$\mathbf{d}_{\mathrm{w}}$	L	*Depth of the foundation (Z-direction)*
	16	$\boldsymbol{L}_{\mathrm{f,x}}$	L	*Semi-length of the foundation in the X-direction*
	17	$\boldsymbol{L}_{\mathrm{f,y}}$	L	*Semi-length of the foundation in the Y-direction*
	18	ω_{i}	1/T	*Circular frequency of the input motion*
Output	19	$\boldsymbol{U}_0 = \boldsymbol{u}_0 / \boldsymbol{A}_0$	-	*Normalised foundation horizontal displacement*
	20	$\boldsymbol{\Phi}_0 = \varphi_0 / \boldsymbol{A}_0$	1/L	*Normalised foundation rotation*
	21	$\bar{\boldsymbol{U}} = \boldsymbol{v}/\boldsymbol{A}_0$	$M^{1/2}$	*Normalised structural modal amplitude*
	22	$\Delta \boldsymbol{U}_{TMD} = \Delta \boldsymbol{u}_{TMD}/\boldsymbol{A}_0$	-	*Normalised TMD horizontal relative displacement*

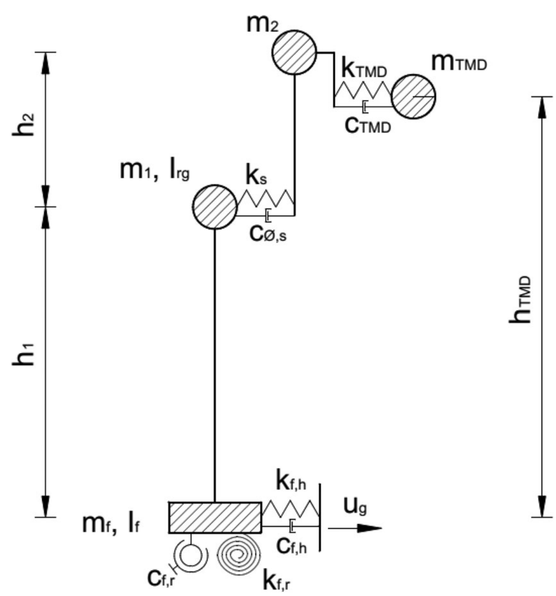

FIGURE 2 Simplified, interpretative model of the soil-structure-TMD system used in the parametric study

3.2 | Interpretative model and validation of the non-dimensional groups

In order to validate the non-dimensional formulation above, the response of a simplified numerical model under harmonic loading of circular frequency ω_{i} was considered, as depicted in Figure 2. The model is formulated to reduce

TABLE 2 Non-dimensional groups of a linear soil-structure-TMD system: (A) model and (B) output parameters

(a) Model parameters	
Non-dimensional groups	**Definition**
G_1. Mass ratio of the TMD	$\boldsymbol{m}_{\mathrm{TMD}}/\boldsymbol{m}_{\mathrm{m}}$
G_2. Frequency ratio of the TMD	$1/\omega_{\mathrm{s}}\sqrt{\boldsymbol{k}_{\mathrm{TMD}}/\boldsymbol{m}_{\mathrm{TMD}}}$
G_3. Damping ratio of the TMD	$\boldsymbol{c}_{\mathrm{TMD}}/2\sqrt{\boldsymbol{m}_{\mathrm{TMD}}\,\boldsymbol{k}_{\mathrm{TMD}}}$
G_4. Normalised TMD height	$\boldsymbol{h}_{\mathrm{TMD}}/\boldsymbol{h}_{\mathrm{m}}$
G_5. Foundation embedment ratio	$\boldsymbol{d}_{\mathrm{w}}/\boldsymbol{L}_{\mathrm{f,x}}$
G_6. Structure-to-soil relative stiffness	$\boldsymbol{h}_{\mathrm{m}}/(\boldsymbol{V}_{\mathrm{s}}\cdot\boldsymbol{T}_{\mathrm{s}})$
G_7. Slenderness ratio	$\boldsymbol{h}_{\mathrm{m}}/\boldsymbol{L}_{\mathrm{f,x}}$
G_8. Soil-structure relative mass	$\boldsymbol{m}_{\mathrm{tot}}/(\boldsymbol{\rho}_{\mathrm{s}}\cdot\boldsymbol{L}_{\mathrm{f,x}}{}^3)$
G_9. Foundation aspect ratio	$\boldsymbol{L}_{\mathrm{f,x}}/\boldsymbol{L}_{\mathrm{f,y}}$
G_{10}. Damping ratio	$\boldsymbol{c}_{\phi\mathrm{s}}/(2\,\omega_{\mathrm{s}}\,\boldsymbol{m}_{\mathrm{m}})$
G_{11}. Effective mass ratio	$\boldsymbol{m}_{\mathrm{m}}/\boldsymbol{m}_{\mathrm{s}}$
G_{12}. Normalised rocking height	$(\boldsymbol{h}_{\mathrm{G,s}}\boldsymbol{m}_{\mathrm{s}}-\boldsymbol{h}_{\mathrm{m}}\boldsymbol{m}_{\mathrm{m}})/[(\boldsymbol{m}_{\mathrm{s}}-\boldsymbol{m}_{\mathrm{m}})\boldsymbol{h}_{\mathrm{m}}]$
G_{13}. Normalised radius of gyration	$\boldsymbol{h}_{\mathrm{m}}^2\boldsymbol{m}_{\mathrm{m}}/(\boldsymbol{r}_{\mathrm{G}}^2\boldsymbol{m}_{\mathrm{s}})-(\boldsymbol{h}_{\mathrm{G,s}}\boldsymbol{m}_{\mathrm{s}}-\boldsymbol{h}_{\mathrm{m}}\boldsymbol{m}_{\mathrm{m}})^2/[\boldsymbol{r}_{\mathrm{G}}^2\boldsymbol{m}_{\mathrm{s}}(\boldsymbol{m}_{\mathrm{m}}-\boldsymbol{m}_{\mathrm{s}})]$
G_{14}. Normalised foundation mass density	$\boldsymbol{\rho}_{\mathrm{c}}\cdot\boldsymbol{h}_{\mathrm{m}}{}^3/\boldsymbol{m}_{\mathrm{m}}$
G_{15}. Normalised frequency	$\omega_{\mathrm{i}}/\omega_{\mathrm{s}}$
(b) Output parameters	
Non-dimensional groups	**Definition**
R_1. Normalised structural deformation	$\boldsymbol{U}=\bar{\boldsymbol{U}}\times\phi(\boldsymbol{h})$
R_2. Normalised TMD displacement	$\boldsymbol{\Delta U}_{\mathrm{TMD}}=\boldsymbol{\Delta u}_{\mathrm{TMD}}(\omega_{\mathrm{i}})/\boldsymbol{A}_0$
R_3. Normalised foundation displacement	$\boldsymbol{U}_0=\boldsymbol{u}_0(\omega_{\mathrm{i}})/\boldsymbol{A}_0$
R_4. Normalised foundation rotation	$\boldsymbol{\Phi}_0\times\boldsymbol{h}_{\mathrm{m}}$

to a simple SDOF with horizontal TMD in case of fixed base, otherwise all the physical parameters listed in Table 1 can be independently varied acting on the components of the system. The model is composed of a mass m_2 placed on top and connected to a lower mass m_1 through the parallel combination of a translational linear spring, having stiffness k_s, and a dashpot, with damping coefficient c_s. The mass m_1, placed at a height h_1, is in turn rigidly connected to the foundation; a rotational inertia I_{rg} is moreover applied at the top of the rigid body. The foundation mass m_f is supported by horizontal and rotational dynamic impedance functions, here calibrated on the solutions proposed by Gazetas.[32] The mass m_2 is equipped with a TMD, whose elevation may range between the ground level ($h_{TMD} = 0$) and the top of the structure ($h_{TMD} = h_1{+}h_2$). This model was implemented in the finite element solver ABAQUS.[34]

In this case, the structural mass is equal to $m_s = m_1{+}m_2$, where m_2 is also the modal mass so that the modal height is simply $h_m = h_1{+}h_2$; accordingly, the barycentre height and the radius of gyration of the structure can be written as $h_{G,s} = (m_1h_1{+}m_2h_m)/m_s$ and $r_g = [(m_1{h_1}^2{+}m_2{h_m}^2{+}I_{rg})/m_s]^{0.5}$. The physical meaning of G_{12} and G_{13} is now more evident: the former represents the height of the structure undergoing rigid motion normalised to the total height, the latter is the ratio between the second moment of mass due to the concentrated mass and the total rotational inertia.

For this simplified soil-structure-TMD system, a fully non-dimensional description of the equation of motion can be derived:

$$\begin{pmatrix} \frac{G_5G_{14}}{G_7^3G_9}+\frac{1-G_{11}}{G_{11}}+1+G_1 & \frac{1-G_{11}}{G_{11}}G_{12}+1+G_1G_4 & 1+G_1 & G_1 \\ Sym & \frac{1-G_{13}}{G_{13}}\left(\frac{1-G_{11}}{G_{11}}G_{12}^2+1\right)+\frac{1-G_{11}}{G_{11}}G_{12}^2+1+G_1G_4^2 & 1+G_1G_4 & G_1G_4 \\ Sym & Sym & 1+G_1 & G_1 \\ Sym & Sym & Sym & G_1 \end{pmatrix}$$

$$\times \begin{pmatrix} R_3 \\ R_4 \\ R_1 \\ R_2 \end{pmatrix} + \begin{pmatrix} c_{fh}/\omega_i m_2 & 0 & 0 & 0 \\ 0 & c_{fr}/\left[\omega_i m_2 (h_1+h_2)^2\right] & 0 & 0 \\ 0 & 0 & 2G_{10}/G_{14} & 0 \\ 0 & 0 & 0 & 2G_1G_2G_3/G_{14} \end{pmatrix} \begin{pmatrix} \dot{R}_3 \\ R_4 \\ \dot{R}_1 \\ \dot{R}_2 \end{pmatrix}$$

$$+ \begin{pmatrix} k_{fh}/\left(\omega_i^2 m_2\right) & 0 & 0 & 0 \\ 0 & k_{fr}/\left[\omega_i^2 m_2 (h_1+h_2)^2\right] & 0 & 0 \\ 0 & 0 & 1/G_{14}^2 & 0 \\ 0 & 0 & 0 & G_1G_2^2/G_{14}^2 \end{pmatrix} \begin{pmatrix} R_3 \\ R_4 \\ R_1 \\ R_2 \end{pmatrix} = \begin{pmatrix} \frac{G_5G_{14}}{G_7^3G_9} + \frac{1-G_{11}}{G_{11}} + 1 + G_1 \\ \frac{1-G_{11}}{G_{11}}G_{12} + 1 + G_1G_4 \\ 1 + G_1 \\ G_1 \end{pmatrix} \sin\tau \qquad (6)$$

where $\tau = \omega_i \times t$ is the normalised time, while m_2, k_s and $h_m = h_1 + h_2$ constitute the reference basis arbitrary chosen to derive all remaining quantities as a function of the non-dimensional groups. The full mathematical development is reported in Appendix A.

The validation of the non-dimensional formulation, here omitted for brevity, consisted of verifying that different configurations of the simplified model characterised by the same non-dimensional groups provide the same response under harmonic loading with varying frequency.

3.3 | Validation on a real case study

The interpretative model of Figure 2 is now validated against the results obtained on a more articulated numerical model, relative to a seven-storey timber building equipped with a Den Hartog-type TMD and tested on a shaking table.[35] Poh'sie et al.[36,37] calibrated a simplified three-dimensional model of the building, called herein 7-masses model, against experimental evidence and more advanced numerical results: it was a lumped mass model in which each floor was modelled as a translational-rotational inertial element connected to the next upper and lower floor by translational and rotational elastic springs. This model was then modified by Gorini and Chisari[31] to account for soil-structure interaction.

The interpretative model proposed in this work was used to reproduce the non-dimensional, TMD performance curve obtained by Gorini and Chisari,[31] shown in Figure 3 with filled circles, relating the TMD effectiveness to the structure-to-soil relative stiffness, group G_6. Consistently with Gorini and Chisari,[31] the TMD effectiveness was defined as $\eta_v = (F_b^{(noTMD)} - F_b^{(TMD)})/F_b^{(noTMD)}$, where F_b is the maximum horizontal inertial force (including the contribution of damping) at the base of the structure and the superscripts TMD and noTMD refer to the structure equipped with and without the TMD, respectively. In light of the above, the validation of the proposed framework includes (1) the identification of

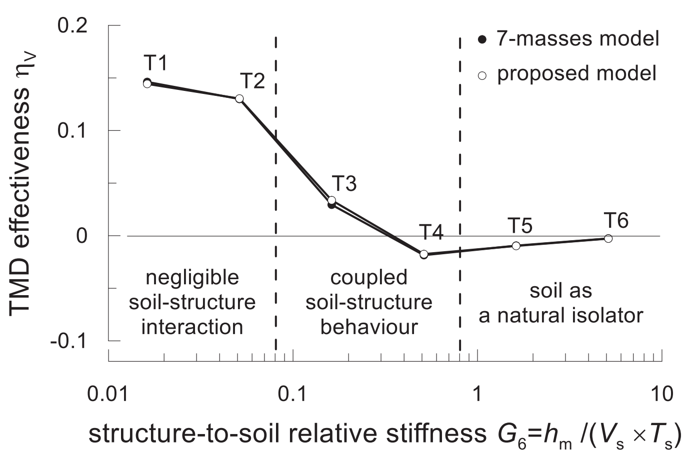

FIGURE 3 Comparison between the TMD effectiveness evaluated with the 7-masses model of the reference timber structure and the proposed interpretative model, varying group $G_6 = 0.02–5.12$

TABLE 3 Derivation of the physical quantities of the simplified model as a function of the non-dimensional groups and of the chosen basis m_2, k_s and $h_m = h_1+h_2$

$\boldsymbol{m}_1 = \frac{1-G_{11}}{G_{11}}\ \boldsymbol{m}_2$
$\boldsymbol{c}_{\phi s} = 2\,G_{10}\sqrt{\boldsymbol{m}_2\,\boldsymbol{k}_s}$
$\boldsymbol{h}_1 = G_{12}\,(\boldsymbol{h}_1 + \boldsymbol{h}_2)$
$\boldsymbol{I}_g = \frac{1-G_{13}}{G_{13}}\ (\boldsymbol{m}_1\,\boldsymbol{h}_1^2 + \boldsymbol{m}_2\,\boldsymbol{h}_m^2) = \frac{1-G_{13}}{G_{13}}\ (\frac{1-G_{11}}{G_{11}}\ G_{12}^2 + 1)\boldsymbol{m}_2\,\boldsymbol{h}_m^2$
$\boldsymbol{m}_{TMD} = G_1\ \boldsymbol{m}_2$
$\boldsymbol{h}_{TMD} = G_4\,(\boldsymbol{h}_1 + \boldsymbol{h}_2)$
$\boldsymbol{k}_{TMD} = G_2^2\ \boldsymbol{k}_s\ \frac{\boldsymbol{m}_{TMD}}{\boldsymbol{m}_2} = G_1\,G_2^2\,\boldsymbol{k}_s$
$\boldsymbol{c}_{TMD} = 2G_3\ \sqrt{\boldsymbol{m}_{TMD}\,\boldsymbol{k}_{TMD}} = 2G_1\,G_2\,G_3\,\sqrt{\boldsymbol{m}_2\,\boldsymbol{k}_s}$
$\boldsymbol{V}_s = \frac{H}{2\pi G_6}\ \sqrt{\frac{\boldsymbol{k}_s}{\boldsymbol{m}_2}}$
$\boldsymbol{L}_{f,x} = (\boldsymbol{h}_1 + \boldsymbol{h}_2)\,/G_7$
$\boldsymbol{L}_{f,y} = \boldsymbol{L}_{f,x}\,/G_9$
$\mathbf{d}_w = G_5\,\boldsymbol{L}_{f,x}$
$\rho_c = \frac{G_{14}\boldsymbol{m}_2}{h_m^3}$
$\boldsymbol{m}_f = 4\,\boldsymbol{d}_w\,\boldsymbol{L}_{f,x}\boldsymbol{L}_{f,y}\,\rho_c = 4\frac{G_5}{G_7^3 G_9}\boldsymbol{H}^3\rho_c$
$\rho_s = \frac{\mathbf{m}_1+\boldsymbol{m}_2+\boldsymbol{m}_f}{L_{f,x}^3 G_8}$

the properties of the interpretative model and (2) the comparison on the dynamic response of the structure, expressed in non-dimensional form, with the 7-masses model.

The physical properties of the timber building are well-documented in Ceccotti et al.[35] and Poh'sie et al.[36,37] The relative non-dimensional groups can be therefore computed according to the expressions in Table 2, that are: $G_1 = 0.012$, $G_2 = 0.977$, $G_3 = 0.075$, $G_4 = 1.376$, $G_5 = 0.125$, $G_6 = 0.016\text{-}5.124$, $G_7 = 3.271$, $G_8 = 3.212$, $G_9 = 0.571$, $G_{10} = 0.041$, $G_{11} = 0.825$, $G_{12} = 0.130$, $G_{13} = 0.955$, $G_{14} = 25.263$. The range of the structure-to-soil relative stiffness, G_6, was defined according to the values used by Gorini and Chisari[31] to determine the TMD performance curve. From this, the equivalent mechanical properties of the proposed, interpretative model were derived through the expressions reported in Table 3, obtained by inverting the equations of the groups.

A steady-state dynamic analysis,[34] providing the steady-state amplitude of the system response due to harmonic excitation, was carried out for six configurations of the proposed model corresponding to different values of G_6, named T1 to T6 in Figure 3, ranging from negligible soil-structure interaction effects ($G_6 < 0.08$) to the condition in which the soil behaves as a natural isolator for the structure ($G_6 > 0.8$).[31,33] The results are shown in Figure 3, demonstrating the ability of the proposed model to simulate the dynamic response of a validated, more articulated numerical representation of the reference soil-structure-TMD system. The TMD loses progressively its effectiveness as the soil-structure interaction effects become appreciable ($G_6 > 0.08$), until producing even a detrimental effect on the structural performance for a very high deformability of the foundation soil compared to the structural one.

It must be pointed out that while the effectiveness evaluated on the total inertial force allows for a fair comparison of different models, it is not very representative of the stress state on a structure in case of damped systems. For this reason, in the following discussion, the effectiveness will be defined based on the internal force, F_s, in the shear spring of stiffness k_s (see Figure 2), which represents the shear force at the base of the structure.

4 | GLOBAL SENSITIVITY ANALYSIS

4.1 | The elementary effect method

With the aim of identifying the most important non-dimensional groups in the response of a linear soil-structure-TMD system, a global sensitivity analysis was carried out by means of the Elementary Effect (EE) Method.[38] The method involves the evaluation of the elementary effect EE_i of the group G_i on the scalar response $\boldsymbol{\eta}$ when G_i is moved of a step Δ_i keeping

TABLE 4 Ranges of variability of the input non-dimensional groups

Group	Range
G_1	0.005-0.05
G_2	Function of G_1
G_3	Function of G_1
G_4	1.0-1.5
G_5	0.1-0.5
G_6	0.0-0.6
G_7	0.5-5.0
G_9	0.1-1.0
G_{10}	0.02-0.1
G_{11}	0.6-1.0
G_{12}	0.0-1.0
G_{13}	0.0-1.0
G_{15}	0-5

the other groups fixed. For the problem at hand, η represents the effectiveness of the TMD in mitigating the maximum base shear F_s in the structure (internal force in the shear spring of stiffness k_s in the model of Figure 2) and is therefore defined as $\boldsymbol{\eta} = \frac{F_s^{(\text{noTMD})} - F_s^{(\text{TMD})}}{F_s^{(\text{noTMD})}}$. The elementary effect therefore reads:

$$\boldsymbol{EE_i(\eta)} = \frac{\eta(G_1, \ldots, G_{i-1}, G_i + \Delta_i, G_{i+1}, \ldots, G_k) - \eta(G_1, \ldots, G_{i-1}, G_i, G_{i+1}, \ldots, G_k)}{\Delta_i} \tag{7}$$

where k is the overall number of groups.

The global sensitivity measure of G_i is the finite distribution F_i composed of all possible EE_i. To represent a EE_i distribution estimated from a sample composed of N_S points, the original formulation proposes the average μ_i and the standard deviation σ_i, where the former is positive if, on average, an increase of G_i leads to an increase of η and negative otherwise. Conversely, the standard deviation σ_i is a measure of the nonlinearity of the effect and the possible interaction with other parameters. Furthermore, Campolongo et al.[39] proposed to use the parameter $\boldsymbol{\mu_i^*} = 1/\boldsymbol{N_S} \sum_{i=1}^{N_S} |\boldsymbol{EE_i}|$. It was therein shown that this quantity represents a good proxy for the total-effect sensitivity index S_{ti}[40] in the Sobol method,[41] that is, the contribution to the total output variance given by the i-th parameter alone and its interactions with other parameters. This allows one to rank parameters, as a large value of $\boldsymbol{\mu_i^*}$ indicates an input with important 'overall' influence on the output.

The N_S different EEs may be computed by different techniques, starting from the original formulation based on trajectories.[38] Here the procedure proposed by Campolongo et al.[42] based on radial One-At-the-Time samples was followed. The method is implemented in the Matlab/Octave toolbox SAFE.[43]

4.2 | Variability of the samples

The ranges of the groups, reported in Table 4, were chosen to account for a large variability in the geometry and mechanical properties of soil-structure systems equipped with a TMD. In design practice, the TMD mass ranges between 0.01 and 0.03 times the mass of the structure while a wider range was used in the sensitivity analysis (G_1 = 0.005-0.05). Groups G_2 and G_3 were considered as dependent on G_1, according to the methodologies proposed by either Den Hartog[2] or Ghosh and Basu.[12] The TMD elevation ranged from the modal height of the first structural mode ($G_4 = 1$) and the top of the structure ($G_4 = 1.5$, considering that, assuming a linear modal shape, the modal height is at about 2/3 the height of the building).

Group G_5 considered realistic cases for the geometric ratio of the foundation. The range for G_6 was defined in accordance with the results obtained by Gorini and Chisari[31] to include cases in which soil-structure interaction is negligible

(G_6 <0.08) or leads to a dynamic response mainly controlled by the compliance of the foundation soil ($G_6 \to 0.6$). As it was shown that G_6 >0.6 leads essentially to uncoupling between the response of soil and that of the structure (soil as natural isolator), a value of 0.6 was considered as upper bound.

The slenderness ratio of the structure included either squat (G_7 close to 0.5) or slender (G_7 close to 5.0) structures, leaving out the case of very tall buildings (G_7 >5.0) for which the assumption of an equivalent SDOF description is no longer acceptable.

The soil density was set equal to $\rho_s = 2.0$ Mg/m^3 as a typical value for soils, while $\rho_c = 2.5$ Mg/m^3 since the foundation is assumed to be a reinforced concrete slab. As a consequence, groups G_8 and G_{14} are not necessary to characterise the system. Both the cases of strip and square foundations were taken into consideration through group $G_9 = 0.1$-1.

Typical values of the damping ratio G_{10}, ranging from 2% to 10%, were considered. Under the assumption of a dynamic response governed by the first vibration mode, the effective mass ratio, G_{11}, was limited to be greater than 0.6. Finally, as seen for the reference model described in Section 3.2, G_{12} and G_{13} ranged from 0 to 1.

4.3 | Analysis settings

The EE method was used to rank the non-dimensional groups based on their impact on the effectiveness η of the system. The maximum amplification factor of the base shear force was evaluated by means of a series of steady-state dynamic analyses by varying G_{15} (normalised input frequency) in the range [0.0, 5.0]. The interpretative model (Figure 2) was perturbed by a harmonic ground motion of unit amplitude at the free node of the horizontal dynamic impedance. To investigate the appropriateness of the fixed-base approximation involved in the design of a TMD, the effectiveness was evaluated considering a fixed base, $\eta_{\mathbf{fixed}}$, or a compliant base, $\eta_{\mathbf{def}}$.

As far as the EE method is concerned, the number of input parameters related to the system configuration are $k = 11$, as G_2, G_3 are considered as a function of G_1, by virtue of the TMD design criteria considered in this study, and G_8 is assumed constant. Considering $N_S = 500$ base sample points, determined by means of Latin Hypercube quasi-random sequence,[42] the total number of evaluations required by the method is $N_S \times (k+1) = 5500$. As mentioned above, the sensitivity analysis was performed on systems in which the groups characterising the TMD, G_2 and G_3, were determined by means of Den Hartog's (DH) or Ghosh and Basu's (GB) method. This latter case implies the determination of the fundamental frequency of the coupled soil-structure system and the application of the same formulas reported for Den Hartog's method using this frequency instead of the structural frequency.

5 | SEISMIC PERFORMANCE OF THE TMD

The results of the sensitivity analysis are aimed at addressing the following points:

a. Identifying the parameters that control the dynamic response of a linear soil-structure-TMD system;
b. Analysing the effects of soil-structure interaction on the seismic performance of TMDs;
c. Identifying the ranges of the non-dimensional groups in which the design criteria at hand lead to an optimised response of the TMD, as well as the ranges in which the TMD has an unfavourable effect on the structural performance.

5.1 | Governing parameters

The EE method is firstly applied to identify the non-dimensional groups that mostly influence the soil-structure-TMD interaction considering DH criterion, configuration named DH TMD. Figure 4A shows the μ^* value for each non-dimensional group computed on the effectiveness $\eta_{\mathbf{fixed}}$ and $\eta_{\mathbf{def}}$, and Figure 4B the relative average μ and standard deviation σ.

As it is expected, the effectiveness of DH TMD on a fixed-base structure is only governed by structural damping, G_{10}, and by the device mass ratio, G_1. When soil-structure interaction is considered, it is evident that the TMD performance is governed by several other factors in addition. Soil-structure interaction partly reduces the influence of the structural damping as a consequence of soil compliance, expressed by the structure-to-soil relative stiffness, G_6. This group controls the dynamic coupling between structure and soil, and its importance for a proper tuning of TMDs was already pointed

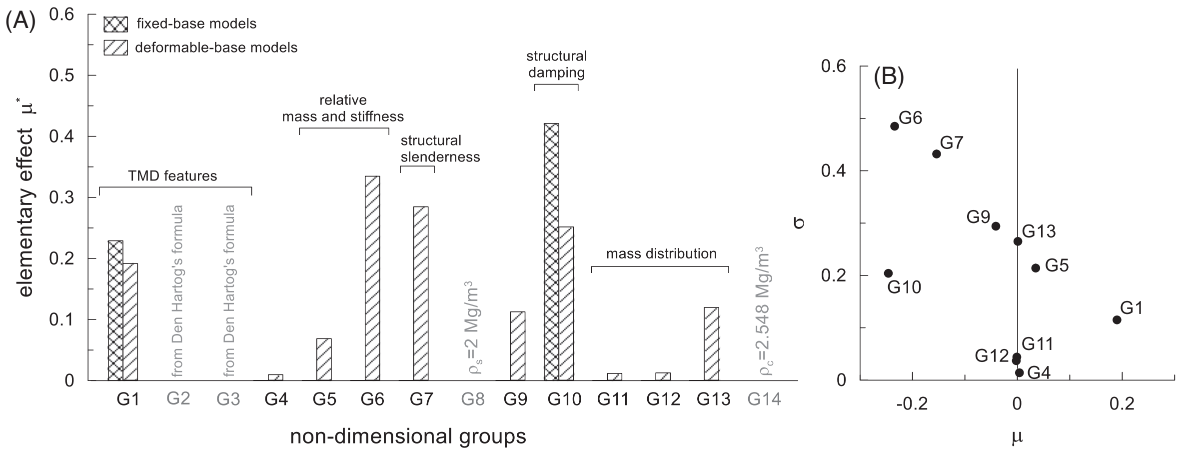

FIGURE 4 Representation of (A) the elementary effect μ^* for each non-dimensional group using Den Hartog's design criterion,[2] and (B) the EEs' relative average μ and standard deviation σ for the deformable-base case

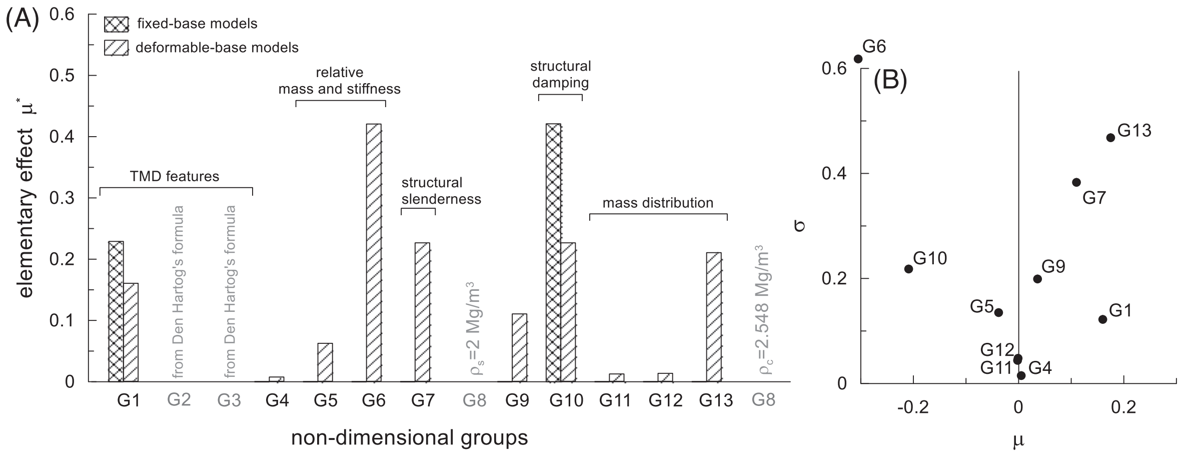

FIGURE 5 Representation of (A) the elementary effect μ^* for each non-dimensional group using Ghosh and Basu's design criterion,[12] and (B) the EEs' relative average μ and standard deviation σ for the deformable-base case

out in some previous works.[10,12,14,31] A significant influence on the TMD performance is also associated with groups G_7, G_9 and G_{13}, which are related to the foundation rocking detuning the response of the translational TMD. The effect of the other groups is instead much more limited.

Figure 4B highlights further characteristics of the groups: among the influential parameters, G_1 has a positive μ value, meaning that increase of the mass ratio produces an increase of the TMD effectiveness, while the opposite holds for G_6, G_7 and G_{10}, that is, stiff structures compared to the foundation soils, slender or highly damped structures are on average less sensitive to the positive effect of the TMD. G_9 and G_{13} have μ close to zero and high σ, meaning that their effect on the effectiveness can be either beneficial or detrimental. In light of the above, it can be deduced that the system parameters governing the effectiveness of a Den Hartog-type TMD are G_1, G_6, G_7, G_9, G_{10}, G_{13}.

In Figure 5, the same procedure is applied to identify the parameters controlling the effectiveness of a TMD designed according to GB criterion, configuration termed GB TMD. The performance of the device is noticeably more affected by the structure-to-soil relative stiffness, even though some other groups, G_7, G_{10}, G_{13}, G_1 and to a minor extent G_9, play a significant role. In the μ-σ plot for GB TMD (Figure 5B), the most relevant differences compared to DH TMD concern G_7 and G_{13}, whose average effect is definitely favourable, indicating that a GB TMD is a more efficient means for controlling vibration in structures with significant rocking deformation modes. The high variability of these effects (high σ) implies correlation with the other parameters.

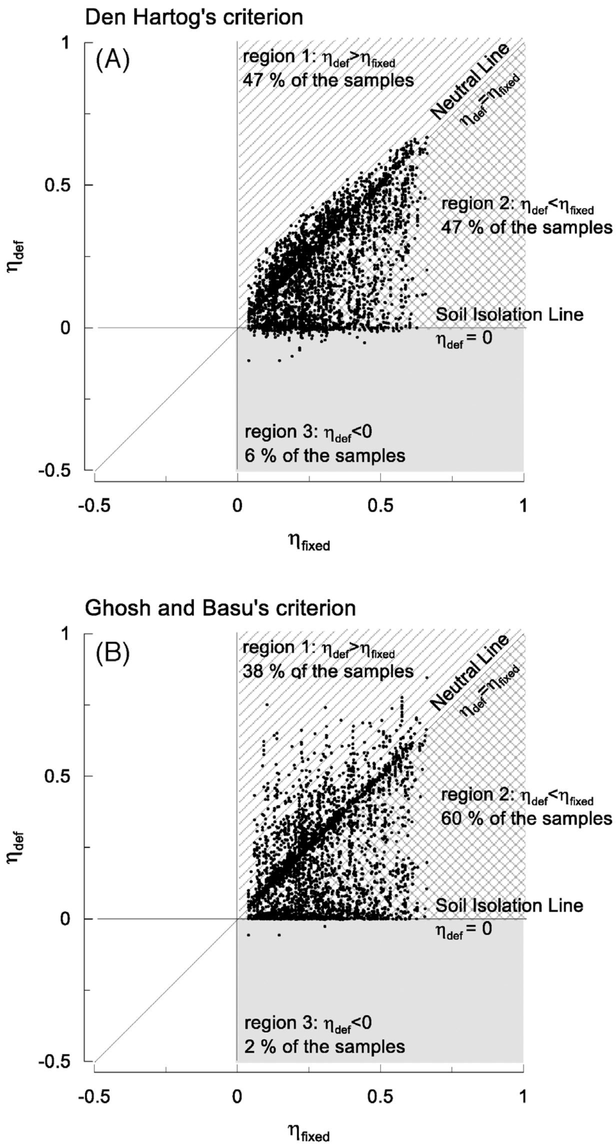

FIGURE 6 Representation of the Tuned Mass Damper (TMD) performance in the plane $\eta_{\mathbf{fixed}}$-$\eta_{\mathbf{def}}$ ($\eta_{\mathbf{fixed}}$ = TMD effectiveness for the fixed-base case; $\eta_{\mathbf{def}}$ = TMD effectiveness for the case with compliant base), using (A) Den Hartog's and (B) Ghosh and Basu's design criteria

5.2 | Features of linear, dynamic soil-structure-TMD interaction

Figure 6A plots the performance points ($\eta_{\mathbf{fixed}}$, $\eta_{\mathbf{def}}$) obtained for all the samples using a DH TMD. As first evidence, all the performance points are located in the semi-plane $\eta_{\mathbf{fixed}} > 0$, indicating that the use of a DH TMD in a structural layout characterised by a predominant mono-modal response and fixed base always reduces the maximum internal forces in the structure. On the contrary, if compliant base is considered, the TMD can assume negative effectiveness $\eta_{\mathbf{def}}$ <0, meaning that neglecting soil-structure interaction in design may worsen the structural performance. Most of the points are located around the so-called Neutral Line $\eta_{\mathbf{def}} = \eta_{\mathbf{fixed}}$ (NL), as it appears evident from the percentage distribution of the samples N/N_{tot} in terms of $\eta_{\mathbf{def}}/\eta_{\mathbf{fixed}}$, shown in Figure 7. The NL is the locus along which the soil-structure interaction has no effect on the TMD performance and determines a boundary between two different behaviours: when $\eta_{\mathbf{def}}/\eta_{\mathbf{fixed}}$ >1 the soil-structure interaction magnifies the TMD performance compared to the fixed-base system (47% of the samples), identifying the so-called Region 1 in the $\eta_{\mathbf{fixed}}$-$\eta_{\mathbf{def}}$ plane, while it reduces the TMD effectiveness when $\eta_{\mathbf{def}}/\eta_{\mathbf{fixed}}$ <1. In the latter case, the TMD partly attenuates structural oscillations as long as $\eta_{\mathbf{fixed}}$ >$\eta_{\mathbf{def}}$ >0 (47% of

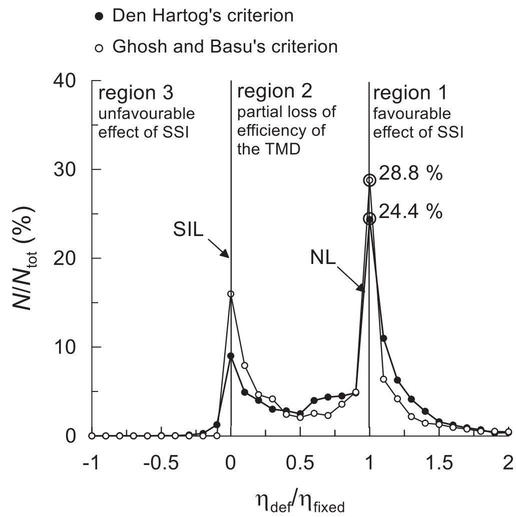

FIGURE 7 Distribution N/N_{tot} of the samples varying the effectiveness ratio $\eta_{\mathbf{def}}/\eta_{\mathbf{fixed}}$

the samples), that is also referred to as Region 2, while it magnifies the response when $\eta_{\mathbf{def}} < 0$ (6%), condition named Region 3.

In Region 1 soil-structure interaction improves the TMD performance because it produces a moderate alteration of the vibration modes of the overall system, exalting the first mode of the fixed-base structure for which the TMD is designed. In Region 2 the structural deformations are partly mitigated by the TMD due to the coupled dynamic response of the soil-structure system causing a more substantial modification of the dynamic response: compared to the fixed-base case, the significant vibration modes of the soil-structure system can be much different and characterised by a combination of translation and rotation. Almost half of the samples exhibits such an intermediate response, in which a Den Hartog-type TMD still appears as a useful solution to control structural vibration, although its performance is no longer optimised. When the performance points belong to the Soil Isolation Line (SIL), $\eta_{\mathbf{def}} = 0$, the soil acts as a natural isolator for the structure and the TMD loses completely its effectiveness, as already demonstrated in some previous works.[12,15,31]

An optimised design of TMDs should aim at moving as many performance points as possible to Region 1. As a first attempt in this direction, a second sensitivity analysis was carried out considering the same samples in which however the design method proposed by Ghosh and Basu[12] was employed. Figure 6B shows the resulting performance points and the relative distribution is depicted in Figure 7. In comparison with DH criterion, there are much less points in Regions 1 and 3, in favour of a larger concentration in Region 2. Consequently, GB criterion appears as a means for reducing the number of critical cases in which soil-structure interaction has a detrimental effect (Region 3), leading however to a structural performance that is globally worse than the response produced by Den Hartog's solution. This can be attributed to the fact that the first mode of vibration of the soil-structure system, used to tune the TMD, may not be a pure structural mode as it may include a combined translational-rotational motion of the foundation, and thus may not be controlled by a translational TMD.

In Figure 8, the two design methods are compared by plotting the performance points in the plane $\eta_{\mathbf{def}}^{DH} - \eta_{\mathbf{def}}^{GB}$, where $\eta_{\mathbf{def}}^{DH}$ and $\eta_{\mathbf{def}}^{GB}$ are the effectiveness of the DH and GB TMDs, respectively, both referred to the case with compliant base. This representation highlights the percentage of samples in which:

- Case 1 (C1): DH criterion is preferable ($\eta_{\mathbf{def}}^{DH} > \eta_{\mathbf{def}}^{GB} > 0$, 65.56% of the samples);
- Case 2 (C2): GB criterion is preferable but DH still achieves some performance gain ($\eta_{\mathbf{def}}^{GB} > \eta_{\mathbf{def}}^{DH} > 0$, 13.55% of the samples);
- Case 3 (C3): the two criteria lead to the same, positive TMD effectiveness ($\eta_{\mathbf{def}}^{GB} = \eta_{\mathbf{def}}^{DH} > 0$, 14.73% of the samples);
- Case 4 (C4): GB criterion should be definitely used in place of DH since the latter has a detrimental effect on the structural performance ($\eta_{\mathbf{def}}^{GB} > 0$ and $\eta_{\mathbf{def}}^{DH} < 0$, 3.98% of the samples);

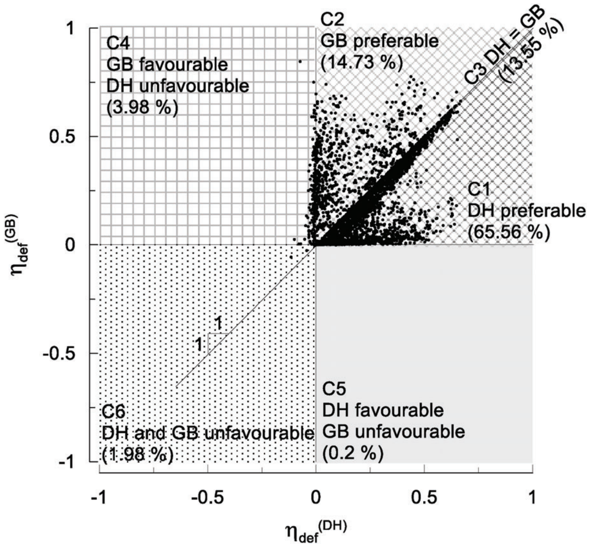

FIGURE 8 Comparison between the Tuned Mass Damper (TMD) effectiveness in a structural system with compliant base obtained using Den Hartog's criterion, $\eta_{\mathbf{def}}^{(\mathbf{DH})}$, and Ghosh and Basu's criterion, $\eta_{\mathbf{def}}^{(\mathbf{GB})}$

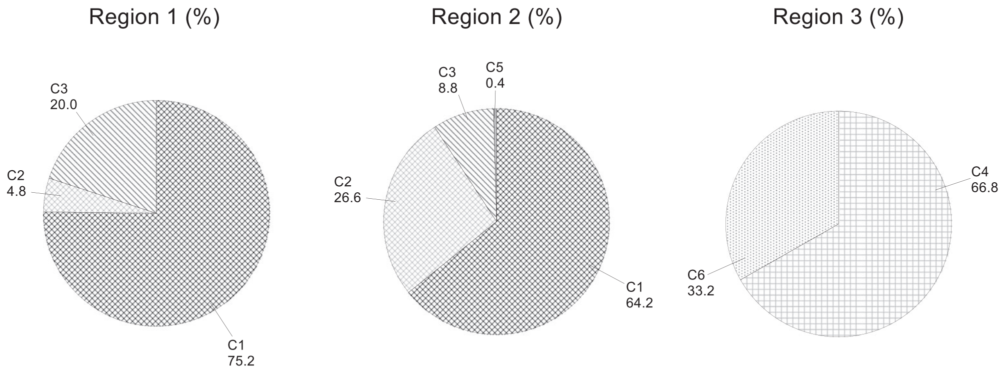

FIGURE 9 Frequency (%) of the cases C1-C6 (see Figure 9) in the performance regions 1, 2 and 3 (see Figure 7)

- Case 5 (C5): DH criterion should be definitely used in place of GB ($\eta_{\mathbf{def}}^{DH} > 0$ and $\eta_{\mathbf{def}}^{GB} < 0$, 0.2% of the samples);
- Case 6 (C6): both methods lead to a performance loss ($\eta_{\mathbf{def}}^{DH} < 0$ and $\eta_{\mathbf{def}}^{GB} < 0$, 1.98% of the samples).

In order to relate the information about the convenience of using DH or GB criterion (Cases 1–6 above) to the alteration of the TMD effectiveness as an effect of soil-structure interaction (Regions 1–3 in Figure 6), Figure 9 illustrates the distribution of the samples for each case in the three TMD performance regions, the latter referring to the distribution obtained with DH criterion (Figure 7A). Regions 1 and 2 are composed of samples in which both DH and GB lead to a positive effectiveness of the TMD. More in detail, the main contribution to Region 1 is given by the samples for which DH is preferable to GB and, to a minor extent, by samples in which the two criteria show the same effectiveness. In Region 2, there is not a marked preference in using one criterion or the other so that the best design strategy should be chosen case by case. As expected, the samples in Region 3 belong to cases 4 and 6; however, in this region both methods are ineffective.

5.3 | Relationship between the TMD performance and the soil-structure layout

The configurations of the soil-structure-TMD system associated with the three performance regions identified above are explored in this section, in order to determine the ranges of the governing parameters that maximise the TMD effectiveness. Figures 10, 11 and 12 show the relative frequency densities of the non-dimensional parameters in Regions 1, 2 and 3, respectively, in which $N_{tot}^{(i)}$ is the total number of samples in Region i and ΔG_j is the amplitude of discretisation of G_j.

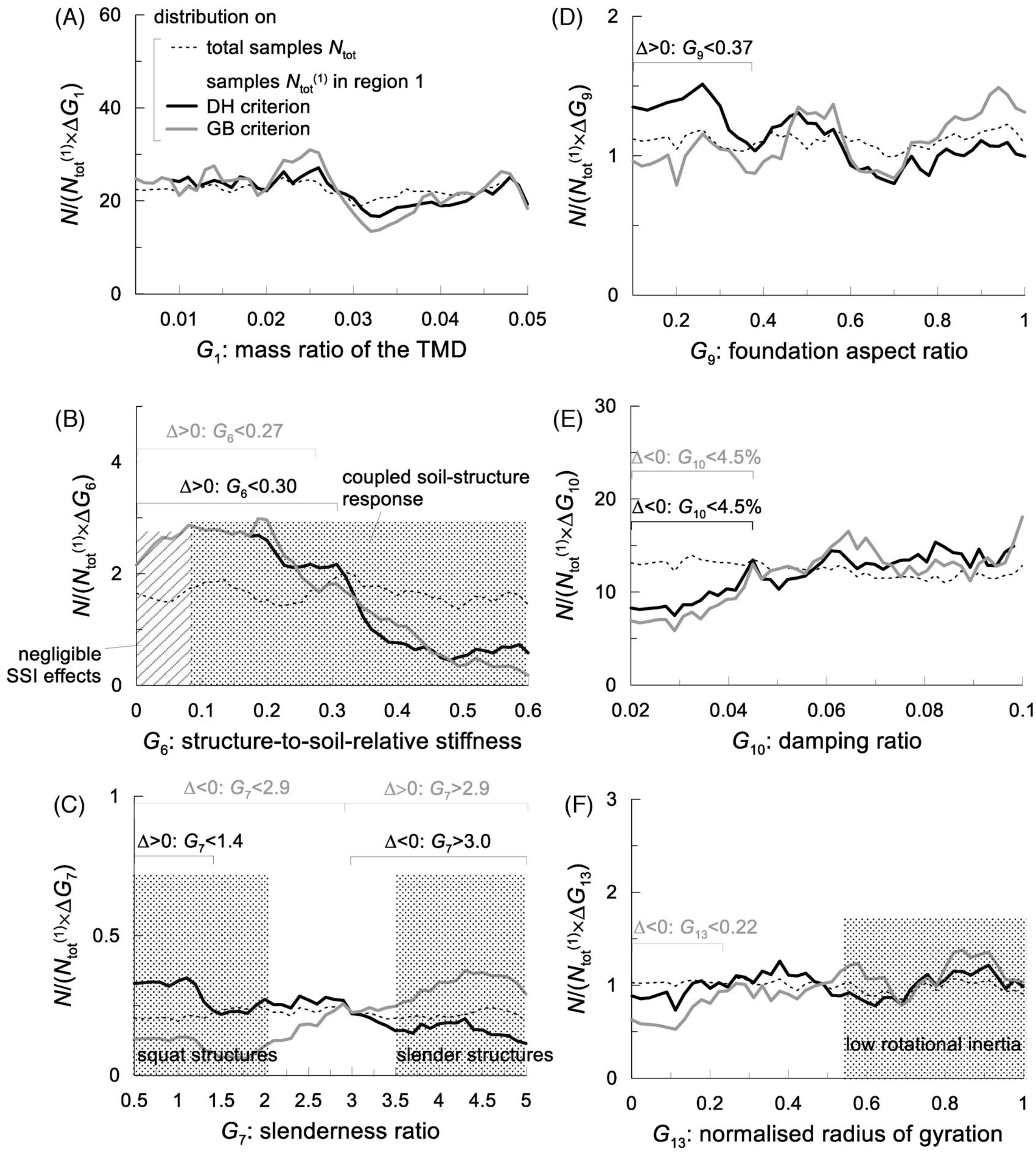

FIGURE 10 Relative frequency density $N/(N_{tot}^{(1)}\times\Delta G_i)$ of the samples $N_{tot}^{(1)}$ in Region 1 (ΔG_i is the amplitude of the class G_i), relative to (A) the mass ratio of the TMD, (b) the structure-to-soil relative stiffness, (C) the slenderness ratio, (D) the foundation aspect ratio, (E) the damping ratio and (F) the normalised radius of gyration

Each plot depicts three curves representing the original random input density of the samples (black dashed line) and the densities of the performance points using DH (thick black line) and GB criteria (thick grey line). The significant ranges of the governing groups for each region are summarised in Tables 5 and 6. They are identified by a marked increment $\Delta>0$ of the performance points with respect to the input random density.

5.3.1 | Region 1: $\eta_{def}/\eta_{fixed} > 1$

Region 1 represents the most favourable condition in which the TMD performance is magnified by soil-structure interaction. In this region, the TMD mass does not appear to have sensitive influence, as seen in Figure 10A. From Figure 10B it can be inferred that the condition $\eta_{def}/\eta_{fixed} > 1$ can be mostly obtained when the structure-to-soil relative stiffness is lower than 0.3, for DH criterion, and 0.27, for GB criterion (negligible soil-structure interaction). A very low number of

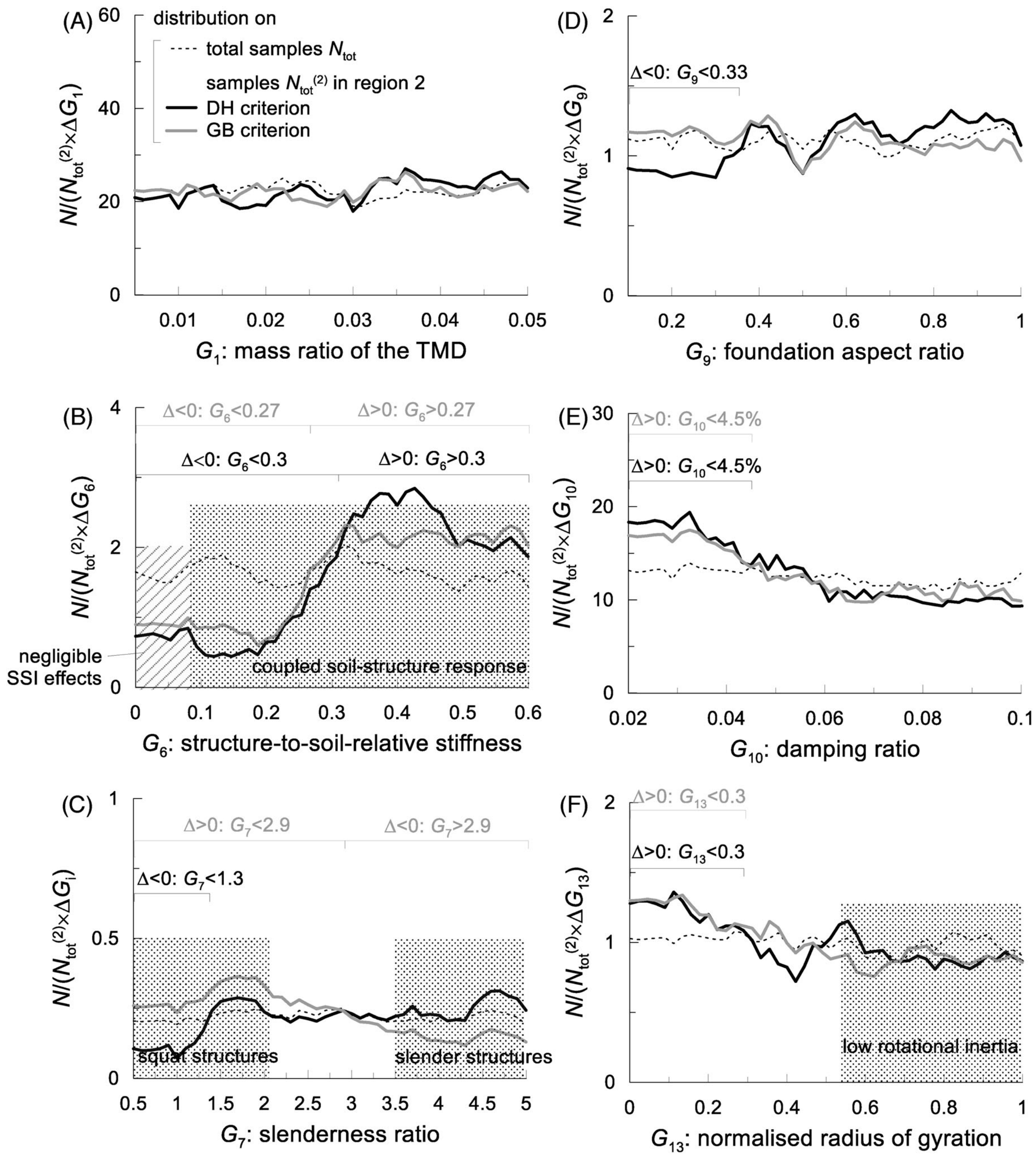

FIGURE 11 Relative frequency density $N/(N_{tot}^{(2)}\times\Delta G_i)$ of the samples $N_{tot}^{(2)}$ in Region 2 (ΔG_i is the amplitude of the class G_i), relative to (A) the mass ratio of the TMD, (B) the structure-to-soil relative stiffness, (C) the slenderness ratio, (D) the foundation aspect ratio, (E) the damping ratio and (F) the normalised radius of gyration

TABLE 5 Significant ranges for the governing parameters using Den Hartog's criterion

Group	Region 1	Region 2	Region 3
G_1. Mass ratio of the TMD	–	–	1.5 - 2.4%
G_6. Structure-to-soil relative stiffness	<0.3	>0.3	>0.46
G_7. Slenderness ratio	<1.4	–	>3.0
G_9. Foundation aspect ratio	<0.37	–	–
G_{10}. Damping factor	–	<4.5 %	–
G_{13}. Normalised radius of gyration	–	<0.3	–

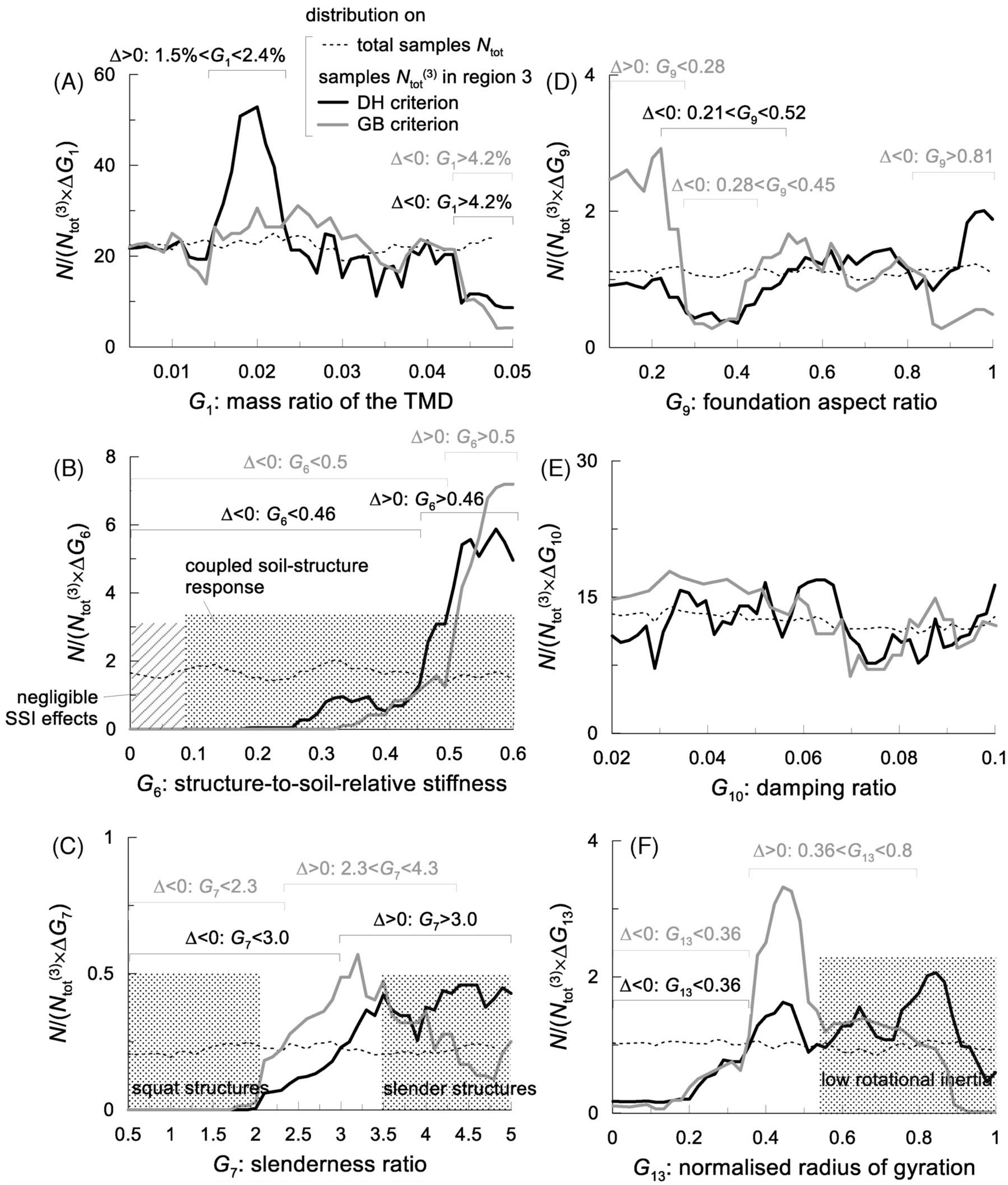

FIGURE 12 Relative frequency density $N/(N_{tot}^{(3)}\times\Delta G_i)$ of the samples $N_{tot}^{(3)}$ in Region 3 (ΔG_i is the amplitude of the class G_i), relative to (A) the mass ratio of the TMD, (B) the structure-to-soil relative stiffness, (C) the slenderness ratio, (D) the foundation aspect ratio, (E) the damping ratio, and (F) the normalised radius of gyration

TABLE 6 Significant ranges for the governing parameters using Ghosh and Basu's criterion

Group	Region 1	Region 2	Region 3
G_1. Mass ratio of the TMD	–	–	–
G_6. Structure-to-soil relative stiffness	<0.27	>0.27	>0.5
G_7. Slenderness ratio	>2.9	<2.9	2.3 - 4.3
G_9. Foundation aspect ratio	–	–	<0.28
G_{10}. Damping factor	–	<4.5%	–
G_{13}. Normalised radius of gyration	–	<0.3	0.36 - 0.8

cases occurs for G_6 >0.3, for which the deformability of the soil becomes predominant compared to the structure deformability.

Focussing on DH criterion, the distribution of the slenderness ratio (Figure 10C) shows that in Region 1 there is a slight concentration of samples for G_7 <1.4, including squat structures, while the number of samples decreases significantly when G_7 >2.9. This again draws attention to the possible negative effect of the structural slenderness on the TMD performance, with possible occurrence of rocking. A completely opposite trend is instead produced by the use of GB criterion, that is, more prone to optimise the TMD performance for slender structures. More specifically, when the fundamental frequency of the soil-structure system is equal to that of the structure with fixed base, GB reduces to DH and accordingly the loss of effectiveness using DH for high G_7 must be ascribed to tuning the TMD to a soil-structure coupled mode of vibration, involving foundation sliding or rocking, that does not necessarily correspond to the mode that magnifies deformations in the structure.

An elongated shape of the foundation in plan (G_9 <0.4) appears preferable to a squared foundation to avoid detuning of a DH TMD in virtue of the higher confining effect of the soil in the transverse plane with respect to the direction of motion.[32]

Definitely, the effectiveness of a DH or GB TMD is maximised mainly in structures characterised by a limited rocking response, resting on foundation soils causing modest soil-structure interaction effects. The last result implies that the fundamental vibration mode of the soil-structure system is mainly translational, so that the TMD can be activated properly.

5.3.2 | Region 2: $0 < \eta_{\mathbf{def}}/\eta_{\mathbf{fixed}} \leq 1$

In most of the cases the TMD effectiveness is partly inhibited by the soil compliance, with ratio $0 < \eta_{\mathbf{def}}/\eta_{\mathbf{fixed}} \leq 1$ (larger structural oscillations than the fixed-base case). In Figure 11 it is evident the concentration of samples for G_6 >0.3, where the compliance of the foundation soil alters the dynamic response of the structure. Other substantial increments of the relative frequency density occur for low values of the structural damping G_{10} and of the normalised radius of gyration G_{13}. The latter refers to structures with high rotational inertia with respect to a centroidal axis, such as structures with large floors or having masses with large eccentricity with respect to the vertical axis. Therefore, a typical soil-structure layout for Region 2 refers to relatively high structure-to-soil relative stiffness, low structural damping and normalised radius of gyration. In these cases, GB criterion presents a higher ability to limit the loss of effectiveness of the device in medium-slender structures (G_7 <2.9) with large rotational inertia.

5.3.3 | Region 3: $\eta_{\mathbf{def}}/\eta_{\mathbf{fixed}} \leq 0$

Region 3 represents the worst condition in which the use of a TMD designed with DH or GB criterion magnifies structural vibration. Only a limited number of cases exhibits such a response. A typical element in this region has a low TMD mass (1.5% < G_1< 2.4% in Figure 12A), high structure-to-soil relative stiffness (Figure 12B) and high slenderness (Figure 12C). A more irregular trend is associated with the other features of the soil-structure layout, G_9, G_{10} and G_{13}. Hence, in Region 3 the device is detuned by the large deformability of the foundation soil compared to the structural one. This feature, combined with a high slenderness of the structure, enhances the rocking response, implying a negative influence of the TMD on the structural performance. In these situations, the use of a translational TMD is therefore not recommended.

6 | CONCLUSIONS

In this paper, a general non-dimensional formulation governing the linear soil-structure-TMD interaction under dynamic conditions was presented based on which an interpretative model was developed. This model, which replaces the more common SDOF system assumed under fixed base conditions, was validated against the results of a more refined numerical model and then employed in an extensive analysis on the performance of TMDs. The discussion was restricted to the case of harmonic ground motion, as an important starting point for more detailed analyses.

The sensitivity analysis indicated that the effectiveness of the TMD is mainly controlled by a limited number of non-dimensional parameters. In addition to the parameters provided by Den Hartog's solution (mass, frequency and damping ratios of the TMD) and the structural damping, there are some other governing factors directly related to soil-structure interaction: the structure-to-soil relative stiffness, the foundation aspect ratio, the slenderness and normalised radius of gyration of the structure.

The results of the sensitivity analysis can be used for a preliminary evaluation of the seismic performance of conventional TMDs in a soil-structure system. Examining the response under various configurations, three regions have been identified, that is, where soil-structure interaction can have a beneficial, neutral or negative effect on the TMD performance. Compared to the fixed-base case, the TMD performance is magnified by soil-structure interaction in layouts characterised by a limited rocking response, such as squat or medium-slender structures, and by a moderate dynamic coupling between the structural and soil responses (Region 1). In these cases, Den Hartog's solution still represents an optimised design criterion and appears preferable to the one proposed by Ghosh and Basu.

Soil-structure interaction has a negative effect on the TMD performance primarily when the soil stiffness is much lower than the structural stiffness (Region 3). In these cases, the dynamic behaviour of the structure is essentially controlled by the foundation soil, with a combined sliding and rotation of the foundation causing a complete detuning of the translational TMD. Nonetheless, in most cases TMD and soil concur to mitigate to a certain extent the internal forces in the structure (Region 2): the TMD loses partially its effectiveness, with structural oscillations greater than those in the fixed-base case, and Den Hartog's criterion can no longer be intended as an optimised solution. These cases refer primarily to structures for which the dynamic interaction with the foundation soil is exalted. In this region, the choice between the two design solutions needs to be evaluated case by case. Therefore, this class of soil-structure systems constitutes the effective target of an optimised design criterion for TMDs, which should be based on the factors governing the performance of the entire soil-structure-TMD system.

DATA AVAILABILITY STATEMENT

The data that support the findings of this study are available from the corresponding author upon reasonable request.

ORCID

Davide Noè Gorini https://orcid.org/0000-0001-6673-0071

REFERENCES

1. Connor JJ. Introduction to structural motion control (1st ed.). *Upper Saddle River*. NJ: Prentice Hall; 2003.
2. Hartog JP Den. *Mechanical Vibrations*. In (eds), New York: Mc-Graw Hill; 1956.
3. Lucchini A, Greco R, Marano G, Monti G. Robust design of tuned mass damper systems for seismic protection of multistory buildings. *J Struct Eng*. 2014;140(8):A4014009.
4. Boccamazzo A, Carboni B, Quaranta G, Lacarbonara W. Seismic effectiveness of hysteretic tuned mass dampers for inelastic structures. *Eng Struct*. 2020;216:110591.
5. Mohebbi M, Joghataie A. Designing optimal tuned mass dampers for nonlinear frames by distributed genetic algorithms. *Struct Des Tall Spec Build*. 2012;21(1):57-76.
6. Pourzeynali S, Salimi S, Kalesar H. Robust multi-objective optimization design of TMD control device to reduce tall building responses against earthquake excitations using genetic algorithms. *Sci Iran*. 2013;20(2):207-221.
7. Poh'sie GH, Chisari C, Rinaldin G, Fragiacomo M, Amadio C. Optimal design of tuned mass dampers for a multi-storey cross laminated timber building against seismic loads. *Earthq Eng Struct Dyn*. 2016;45(12):1977-1995.
8. Poh'sie GH, Chisari C, Rinaldin G, Fragiacomo M, Amadio C, Ceccotti A. Application of a translational tuned mass damper designed by means of genetic algorithms on a multistory cross-laminated timber building. *J Struct Eng*. 2016;142(4):E4015008.
9. Salvi J, Rizzi E, Rustighi E, Ferguson NS. Optimum tuning of passive tuned mass dampers for the mitigation of pulse-like responses. *ASME J Vib Acoust*. 2018;140(6):061014. https://doi.org/10.1115/1.4040475
10. Wu J, Chen G, Lou M. Seismic effectiveness of tuned mass dampers considering soil-structure interaction. *Earthq Eng Struct Dyn*. 1999;28(11):1219-1233.
11. Takewaki I. Soil-structure random response reduction via TMD-VD simultaneous use. *Comput Methods Appl Mech Eng*. 2000;190(5-7):677-690.
12. Ghosh A, Basu B. Effect of soil interaction on the performance of tuned mass dampers for seismic applications. *J Sound Vib*. 2004;274(3-5):1079-1090.
13. Wong HL, Luco JE. *Tables of Impedance Functions and Input Motions for Rectangular Foundations*. Los Angeles, CA: Dept. of Civ. Engrg., Univ. of Southern California; 1978. Report CE-78-15.
14. Liu MY, Chiang WL, Hwang JH, Chu CR. Wind-induced vibration of high-rise building with tuned mass damper including soil-structure interaction. *J Wind Eng Ind Aerodyn*. 2008;96:1092-1102.

15. Wolf JP. *Foundation Vibration Analysis Using Simple Physical Models*. Englewood Cliffs, NJ: Prentice-Hall; 1994.
16. Farshidianfar A, Soheili S. Ant colony optimization of tuned mass dampers for earthquake oscillations of high-rise structures including soil-structure interaction. *Soil Dyn Earthq Eng*. 2013;51(1):14-22.
17. Farshidianfar A, Soheili S. ABC optimization of TMD parameters for tall buildings with soil structure interaction. *Interact Multiscale Mech*. 2013;6(4):339-356.
18. Farshidianfar A, Soheili S. Optimization of TMD parameters for earthquake vibrations of tall buildings including soil structure interaction. *Int J Optim Civil Eng*. 2013;3(3):409-429.
19. Bekdas G, Nigdeli SM. Metaheuristic based optimization of tuned mass dampers under earthquake excitation by considering soil-structure interaction. *Soil Dyn Earthq Eng*. 2017;92:443-461.
20. Salvi J, Pioldi F, Rizzi E. Optimum tuned mass dampers under seismic soil-structure interaction. *Soil Dyn Earthq Eng*. 2018;114:576-597.
21. Wang JF, Lin CC. Seismic performance of multiple tuned mass dampers for soil irregular building interaction systems. *Int J Solids Struct*. 2005;42(20):5536-5554.
22. Li C, Yu Z, Xiong X, Wang C. Active multiple-tuned mass dampers for asymmetric structures considering soil-structure interaction. *Struct Control Health Monit*. 2009;17(4):452-472.
23. Li C. Effectiveness of active multiple-tuned mass dampers for asymmetric structures considering soil-structure interaction effects. *Struct Des Tall Spec Build*. 2010;21(8):543-565.
24. Jabary RN, Madabhushi SPG. Tuned mass damper effects on the response of multi-storied structures observed in geotechnical centrifuge tests. *Soil Dyn Earthq Eng*. 2015;77:373-380.
25. Madabhushi SPG. *Centrifuge Modelling for Civil Engineers*. Taylor Francis, ISBN; 2014. 978-0415668248.
26. De Angelis M, Perno S, Reggio A. Dynamic response and optimal design of structures with large mass ratio TMD. *Earthq Eng Struct Dyn*. 2012;41:41-60. https://doi.org/10.1002/eqe.1117
27. Matta E. A novel bidirectional pendulum tuned mass damper using variable homogeneous friction to achieve amplitude-independent control. *Earthq Eng Struct Dyn*. 2019;48:653-677. https://doi.org/10.1002/eqe.3153
28. Deastra P, Wagg D, Sims N, Akbar M. Tuned inerter dampers with linear hysteretic damping. *Earthq Eng Struct Dyn*. 2020;49:1216-1235. https://doi.org/10.1002/eqe.3287
29. Pietrosanti D, De Angelis M, Basili M. Optimal design and performance evaluation of systems with Tuned Mass Damper Inerter (TMDI). *Earthq Eng Struct Dyn*. 2017;46:1367-1388. 10.1002/eqe.2861
30. Xiang Y, Koetaka Y, Nishira K. Steel frame with aseismic floor: from the viscoelastic Decoupler model to the elastic structural response. *Earthq Eng Struct Dyn*. 2021;50:1651-1670. https://doi.org/10.1002/eqe.3419
31. Gorini DN, Chisari C. Effect of soil-structure interaction on seismic performance of Tuned Mass Dampers in buildings. In Earthquake Geotechnical Engineering for Protection and Development of Environment and Constructions: *Proceedings of the 7th International Conference on Earthquake Geotechnical Engineering, (ICEGE 2019)*, Rome. 2019:2690-2697; 10.1201/9780429031274
32. Gazetas G. Foundation vibrations. *In* Fang H-Y (eds), *Van Nostrand Reinhold, Foundation Engineering Handbook*. New York, Q6 NY: Springer:553-593; 1991.
33. Veletsos AS, Nair VV. Seismic interaction of structures on hysteretic foundations. *J Struct Eng ASCE*. 1975;101(1):109-129.
34. Systemes Dassault. *ABAQUS 6.12-1 Documentation*. Providence, RI: Dassault Systémes; 2013.
35. Ceccotti A, Sandhaas C, Okabe M, Yasumura M, Minowa C, Kawai N. SOFIE project - 3D shaking table test on a seven-storey full-scale cross-laminated timber building. *Earthq Eng Struct Dyn*. 2013;42(13):2003-2021.
36. Poh'sie GH, Chisari C, Rinaldin G, Fragiacomo M, Amadio C. Optimal design of tuned mass dampers for a multi-storey cross laminated timber building against seismic loads. *Earthq Eng Struct Dyn*. 2016;45(12):1977-1995.
37. Poh'sie GH, Chisari C, Rinaldin G, Fragiacomo M, Amadio C, Ceccotti A. Application of a translational Tuned Mass Damper designed by means of genetic algorithms on a multistory cross-laminated timber building. *J Struct Eng*. 2016b;142(4):E4015008.
38. Morris M. Factorial sampling plans for preliminary computational experiments. *Technometrics*. 1991;33(2):161-174.
39. Campolongo F, Cariboni J, Saltelli A. An effective screening design for sensitivity analysis of large models. *Environ Model Softw*. 2007;22:1509-1518.
40. Homma T, Saltelli A. Importance measures in global sensitivity analysis of Nonlinear Models. *Reliab Eng Syst Saf*. 1996;52:1-17.
41. Sobol IM. Sensitivity estimates for nonlinear mathematical model. *Math Model Comput Exp*. 1993;1:407-414.
42. Campolongo F, Saltelli A, Cariboni J. From screening to quantitative sensitivity analysis: a unified approach. *Comput Phys Commun*. 2011;182:978-988.
43. Pianosi F, Sarrazin F, Wagener T. A Matlab toolbox for global sensitivity analysis. *Environ Model Softw*. 2015;70:80-85.

How to cite this article: Gorini DN, Chisari C. Impact of soil-structure interaction on the effectiveness of Tuned Mass Dampers. *Earthquake Engng Struct Dyn*. 2022; 1–21. https://doi.org/10.1002/eqe.3625

APPENDIX A
NON-DIMENSIONAL EQUATION OF MOTION

The equation of motion for the simplified soil-structure-TMD system introduced in Section 3.2 reads:

$$\begin{pmatrix} m_f + m_1 + m_2 + m_{TMD} & m_1 h_1 + m_2 (h_1 + h_2) + m_{TMD} h_{TMD} & m_2 + m_{TMD} & m_{TMD} \\ Sym & I_f + I_{rg} + m_1 h_1^2 + m_2 (h_1 + h_2)^2 + m_{TMD} h_{TMD}^2 & m_2 (h_1 + h_2) + m_{TMD} h_{TMD} & m_{TMD} h_{TMD} \\ Sym & Sym & m_2 + m_{TMD} & m_{TMD} \\ Sym & Sym & Sym & m_{TMD} \end{pmatrix} \begin{pmatrix} \ddot{u}_0 \\ \ddot{\varphi}_0 \\ \ddot{u}_2 \\ \Delta\ddot{u}_{TMD} \end{pmatrix}$$

$$+ \, diag\left(k_{fh} \quad k_{fr} \quad k_s \quad k_{TMD} \right) \begin{pmatrix} u_0 \\ \varphi_0 \\ u_2 \\ u_{TMD} \end{pmatrix} = - \begin{pmatrix} m_f + m_1 + m_2 + m_{TMD} \\ m_1 h_1 + m_2 (h_1 + h_2) + m_{TMD} h_{TMD} \\ m_2 + m_{TMD} \\ m_{TMD} \end{pmatrix} \ddot{u}_g \tag{8}$$

In order to derive a non-dimensional form of Equation 8, the quantities m_2, ω_i and $h_m = h_1 + h_2$ are arbitrary chosen to constitute the reference basis (quantities containing the three fundamental physical dimensions of the problem that are length, mass and time). The remaining quantities are uniquely determined as a function of the non-dimensional groups, as reported in Table 3. These expressions can be substituted into Equation 8:

$$\begin{pmatrix} \frac{G_5}{G_7^3 G_9} \frac{H^3 \rho_c}{m_2} + \frac{1 - G_{11}}{G_{11}} + 1 + G_1 & \frac{1 - G_{11}}{G_{11}} G_{12} + 1 + G_1 G_4 & 1 + G_1 & G_1 \\ Sym & \frac{1 - G_{13}}{G_{13}} \left(\frac{1 - G_{11}}{G_{11}} G_{12}^2 + 1 \right) + \frac{1 - G_{11}}{G_{11}} G_{12}^2 + 1 + G_1 G_4^2 & 1 + G_1 G_4 & G_1 G_4 \\ Sym & Sym & 1 + G_1 & G_1 \\ Sym & Sym & Sym & G_1 \end{pmatrix}$$

$$\times \begin{pmatrix} \ddot{U}_0 \\ H\ddot{\phi}_0 \\ \ddot{U}_2 \\ \boldsymbol{\Delta}\ddot{U}_{TMD} \end{pmatrix} + \begin{pmatrix} \frac{c_{fh}}{m_2} & 0 & 0 & 0 \\ 0 & \frac{c_{fr}}{(m_2 H^2)} & 0 & 0 \\ 0 & 0 & 2G_{10}\sqrt{\frac{k_s}{m_2}} & 0 \\ 0 & 0 & 0 & 2G_1 G_2 G_3 \sqrt{\frac{k_s}{m_2}} \end{pmatrix} \begin{pmatrix} \dot{U}_0 \\ H\dot{\phi}_0 \\ \dot{U}_2 \\ \boldsymbol{\Delta}\dot{U}_{TMD} \end{pmatrix}$$

$$+ \begin{pmatrix} \frac{k_{fh}}{m_2} & 0 & 0 & 0 \\ 0 & \frac{k_{fr}}{(m_2 H^2)} & 0 & 0 \\ 0 & 0 & \frac{k_s}{m_2} & 0 \\ 0 & 0 & 0 & G_1 G_2^2 \frac{k_s}{m_2} \end{pmatrix} \begin{pmatrix} U_0 \\ H\phi_0 \\ U_2 \\ \boldsymbol{\Delta}U_{TMD} \end{pmatrix} = \begin{pmatrix} \frac{G_5}{G_7^3 G_9} \frac{H^3 \rho_c}{m_2} + \frac{1 - G_{11}}{G_{11}} + 1 + G_1 \\ \frac{1 - G_{11}}{G_{11}} G_{12} + 1 + G_1 G_4 \\ 1 + G_1 \\ G_1 \end{pmatrix} \omega_i^2 \mathbf{sin}\,(\omega_i t) \tag{9}$$

A fully non-dimensional formulation of the equation of motion can be finally obtained by normalising time as $\tau = \omega_i \times t$ and dividing both members of Equation 9 by ω_i^2, giving Equation 6 shown in Section 3.2.